Computational Fluid Dynamics modeling of Savonius type vertical axis water rotor: Assessment of meshing dimensions and comparison with experiments

Ibrahim MABROUKI[(1)], Abdelkader DJERAD[(2*)], Mohamed OMRI[(1)], Zied DRISS[(1)], Mohamed Salah ABID[(1)]

[(1)]Laboratory of Electro-Mechanic Systems (LASEM), National School of Engineers of Sfax (ENIS), University of Sfax, B.P. 1173, Road Soukra km 3.5, 3038 Sfax, TUNISIA

[(2)]Department of mathematics, University of M'Sila, Bordj Bou Arreridj road, M'Sila 28000, ALGERIA

[(*)]Corresponding author: abdelkader.djerad@univ-msila.dz

Abstract

In this paper, we are interested in studying the hydrodynamic behavior of the Savonius rotors installed in a water channel. We performed a comparison of four different numbers of nodes and cells. A Hexahedral type is used. The finite volume method was employed to solve the Unsteady Navier-Stokes equations governing the transport of momentum. The present numerical observations reasonably, describe the numerical simulation of a Savonius-type vertical axis water turbine. The comparison with experimental results obtained from literature presents a good agreement.

Key word: Savonius rotor, CFD, RANS, URANS.

1. Introduction

The awareness of the rising level of global warming, global warming and rising in fossil fuel prices resulted in investigations of water turbine technologies. While the water the rotor come into configurations vertical axes and horizontal axis, vertical axis the rotor water are much more common as small rotor where the omni-directionality and reduces noise become pronounced. Water vertical rotor axes are most prospects of all the water technology for the production of small-scale energy in the built environment. In wide applications, the quality of energy efficiency is of paramount importance because an investigation by Shamshir band, and Para. Axis vertical selection of the water for the rotor field defined in the built environment will depend on various factors such as the speed of the water, blade designs, sitting arrangements, weight, components of the energy conversion systems water, etc..The inclined axis rotors are used as power converters smaller river. [2] Vermaaket al.[4]reviewing

the state of the art technology of micro small scale hydrokinetic river as horizontal axis and vertical axis rotor water and found that the main barrier to the use of this technology in areas particularly rural ones is the lack of research in the economic, technical domains and environmental benefits of these technologies. The subject is considered in the preliminary phase of the research, but there are some experimental units and installation-oriented research in some countries. Companies such as Throptom Energy Services(UK), Alternative Hydro Solutions Ltd.(Canada), Lucid Energy Technologies(USA), Seabell Int. Co., fabricated and installed prototypes of tidal rotor that are either in the business sector or in the research stage. [5]Tidal rotor technology has not been widely used commercially because of limitations because the initial installation cost, but it got great potential to provide power even with low speed. Because of the high cost of rotor to harness the currents of water, it is important to choose a rotor having optimum efficiency at the scene selected. In this theme, Ramos and Iglesius[6] presented a parametric approach to evaluate the performance of individual water rotoras Gorlovhelical rotor and Evapodinto their case study applied to a coastal bay NWS pain. Carballo and Iglesius[7] studied the energy converter of hydro electric power efficiency integrating the task of characterization of wave resource at a given site with the computation of the power performance that was previously considered disconnected. Energy produced is generally lower for the rotor to be installed in arrays but may be installed where the speed of the free power is equal to or greater than 0.5m/s. [5] Malipeddiand Chatterjee[8]performed a study to calculate the effect of the geometry of the duct on performance of a tidal Darrieus. They found that the geometry of the outer sheath with a straight shape is greater with respect to a convex outer conduit as regards the power coefficient(Cp). Pontaand Dutt[9]did a study on the performance of a Darrieus hydrokinetic turbine by increasing the fluid circulation incident from the turbine by incorporating a channeling device. The rotors are primarily intended for the production of small-scale energy. A major turbine of its kind is the tidal Savonius that has the ability to self-start at a very low fluid velocity[10]. Golecha et al.[11]have conducted an experiment to optimize the position of the baffle plate in the upstream of a hydrokinetic Savonius rotor to maximize power generated by the rotors. The literature shows the potential of vertical axis Savonius rotor type for producing energy in the form of small scale micro tidal. However, there is little research on the evaluation of the performance of the basic design for different conditions in low speed even if the water got some unique properties such as higher specific weight than air momentum for same speed etc.

The objective of the study is to calculate study of tidal Savonius the rotor once the CFD model is validated by comparing the results of calculation and experimental velocity profiles. In the present paper, we are interested of the hydrodynamic behavior of the Savonius rotors installed in a water channel. We performed a comparison of four different numbers of nodes and cells.

2. Geometry configuration

The goal of this section is to demonstrate various meshing capabilities of “Fluent” allowing us to better adjust the computational mesh to the problem at hand. Although, the automatically generated mesh is usually appropriate, intricate problems with thin and/or small. Important, geometrical and physical features can result in extremely high number of cells, for which the computer memory is too small. In such cases, «Fluent” options allow us to manually adjust the computational mesh to the solved problem's features to resolve them better. Figure 1 presents the meshing of the test bench with some parameters like the number and the type of cells. Table 1 summarized all information about meshing. It consists of four different numbers of nodes and cells. A Hexahedral type is used for the cells

Mesh	Total of nodes	Total of cells	Type of cells
a	11961	9728	Hexahedral
b	139426	129336	
c	491308	461922	
d	1115216	1064015	

Tab. 1Information about meshing

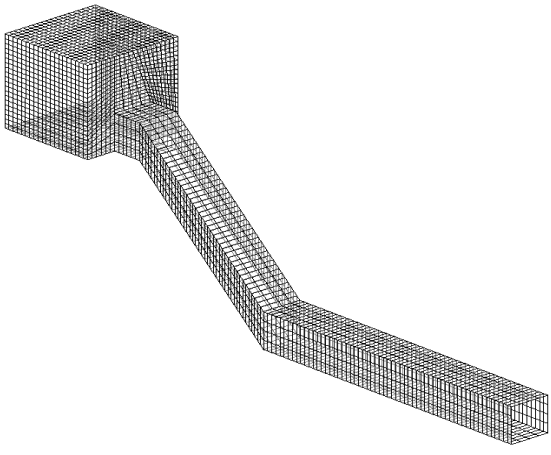

(a) 9728 Cells

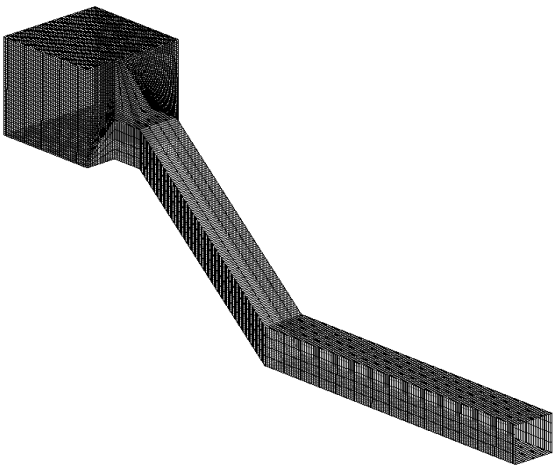

(b) 129336 Cells

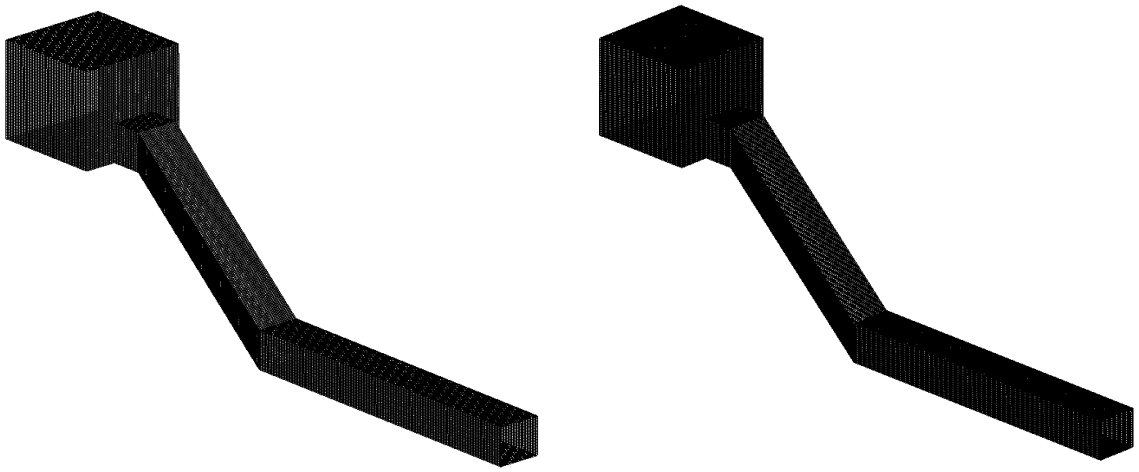

(c) 461922Cells (d) 1064015 Cells

Fig. 1 Different dimensions of mesh cells (3-D view)

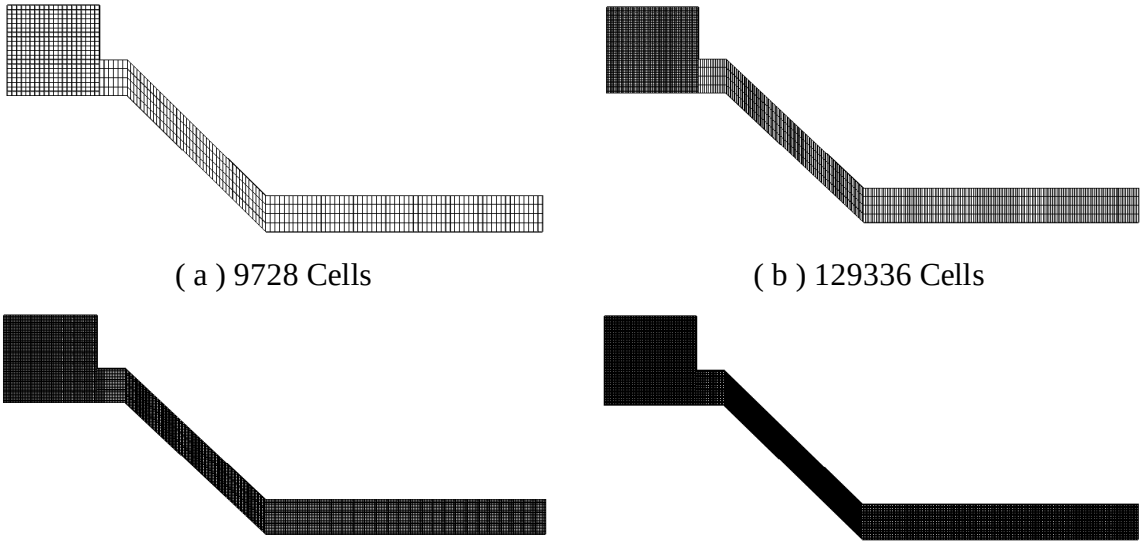

(a) 9728 Cells (b) 129336 Cells

(c) 461922 Cells (d) 1064015 Cells

Fig. 2 Different dimensions of mesh cells (2-D view)

3. Numerical results

3.1. Volume fraction

Figures3,4,5 and 6 show the distribution of the volume fraction of water in the test section bench on the transverse plane defined by z = 0.5 m for the four cases of number of meshing cells for different instances of the water flow. According to these results, it has been observed that when the control gate is opened an outlet of water starts to flow from the intake. In these conditions, it has been observed that when we refine the meshing, the phases become discredited. With a small number of cells as shown in the first two cases, it has been observed

several volume fractions between air (volume fraction equal to 0) and water (volume fraction equal to 1). The turbulence phenomenon is the highest as the mesh number is the lowest. Moreover, it has been observed a discontinuity in phases for the lowest mesh number. Indeed, the waterfront and the water thickness are the longest and the highest respectively for the fourth case. The water flow ahead through the penstock. Also, in our simulation, the water height is very low in the test section bench. The turbulence phenomenon appears only in the intake during the flow. The best result regarding precision is found for 1.064015 cells.

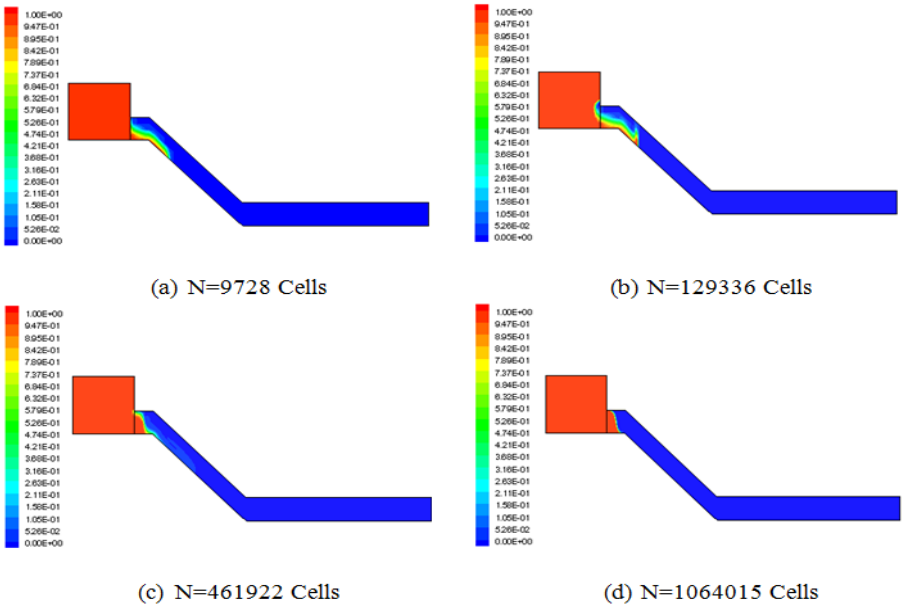

Fig. 3Distribution of the volume fraction in the plane z=0.5 m at t=0.1 s

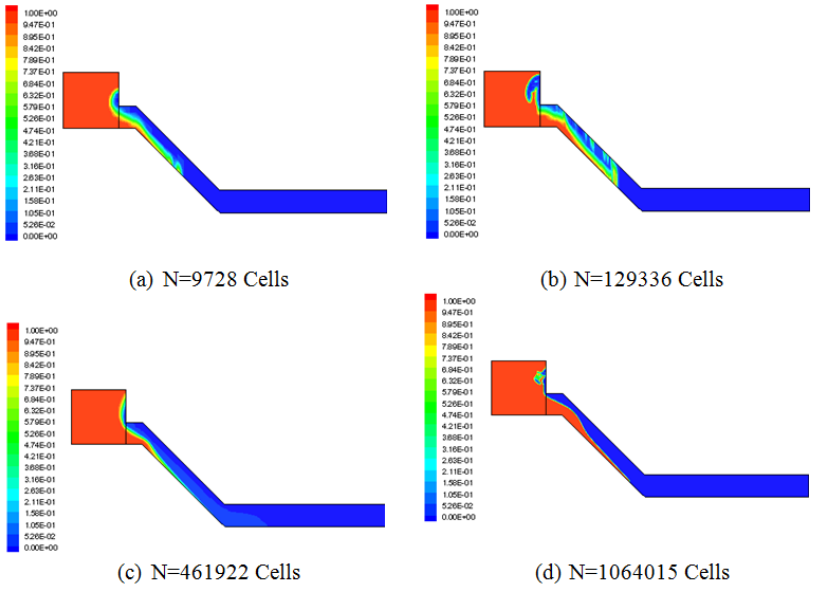

Fig. 4Distribution of the volume fraction in the plane z=0.5 m at t=0.6 s

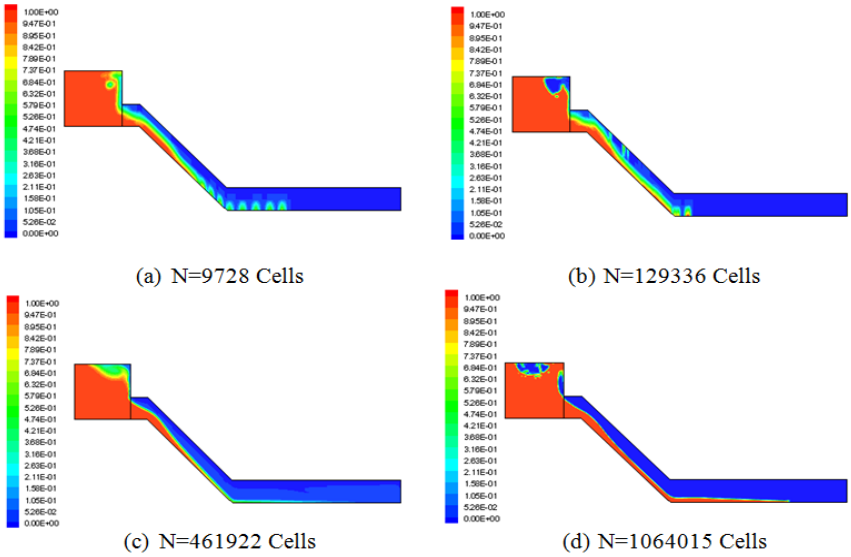

Fig. 5Distribution of the volume fraction in the plane z=0.5 m at t=1 s

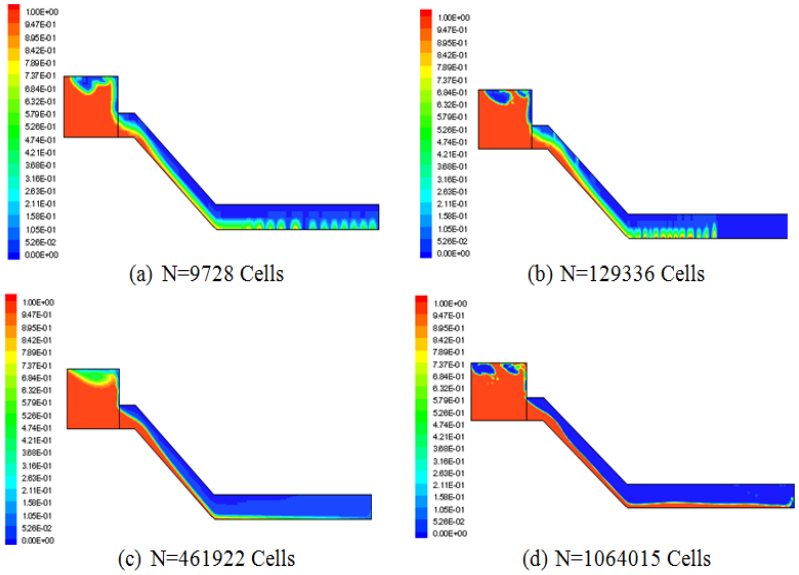

Fig. 6Distribution of the volume fraction in the plane z=0.5 m at t=1.4 s

3.2. Static Pressure

Figures 7, 8, 9 and 10 show the distribution of the static pressure in the test bench on the transverse plane defined by z=0.5 m for the four case of meshing number and for different instances of the water flow. The static pressure is defined as the pressure exerted by a still liquid or gas, especially water when the bodies on which the pressure was exerted are not in motion. According to these results, it has been observed that a compression zone is located in

the bottom of the tank and in the top of the intake. Then the static pressure decrease all over the penstock and the test section defining a zone of depression characteristic of minimum values for the three first cases, unlike the fourth case in which the passage from maximum values to minimum values is smoother. It has been noted also that the static pressure is decreasing during the time. This could be explained by the fact that since water had been moving, its level in the tank had decreased and so did the static pressure.

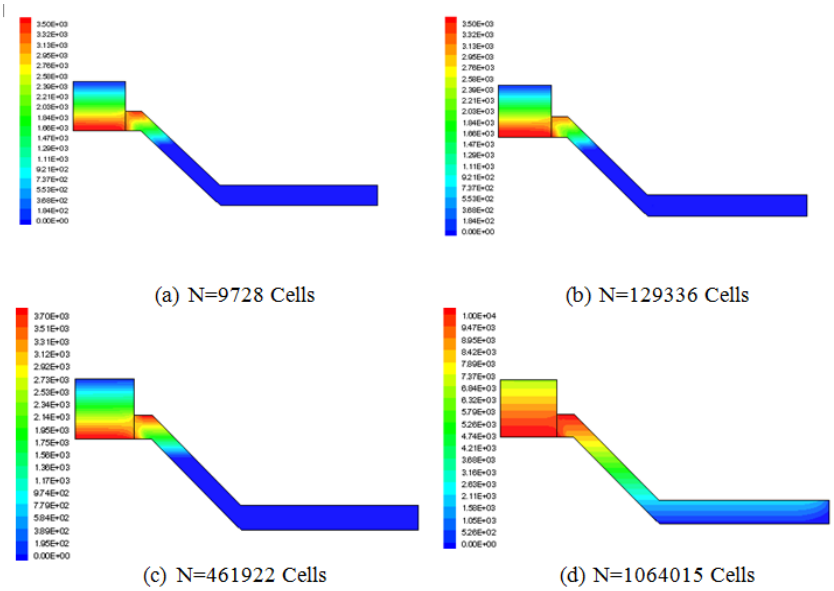

Fig.7Distribution of the static pressure in the plane z=0.5 m at t=0.1 s

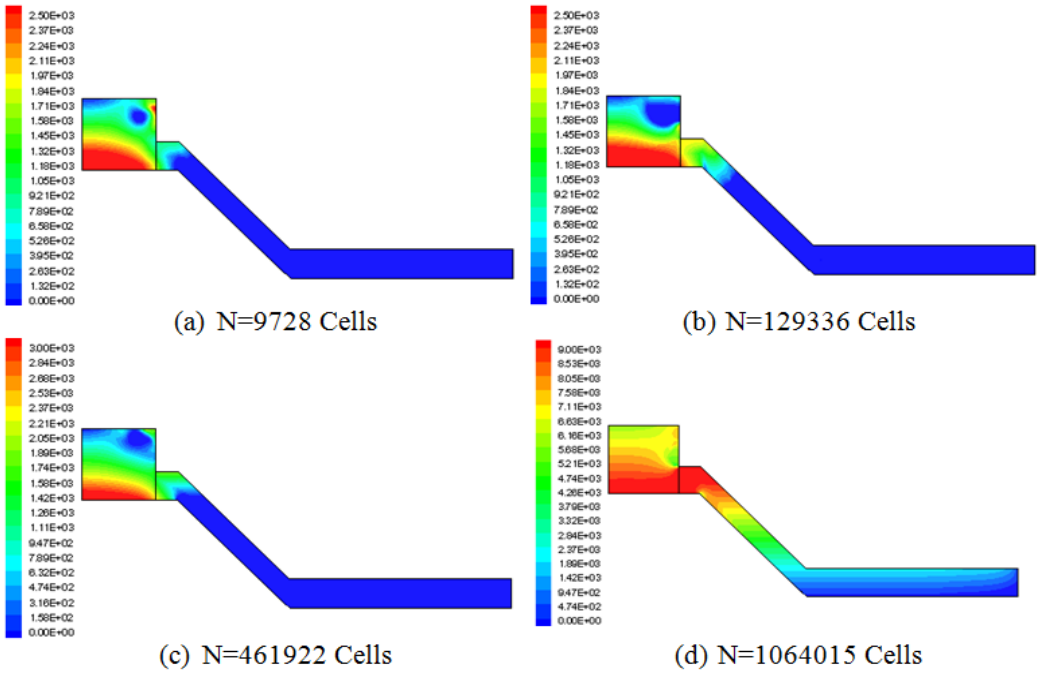

Fig.8Distribution of the static pressure in the plane z=0.5 m at t=0.6 s

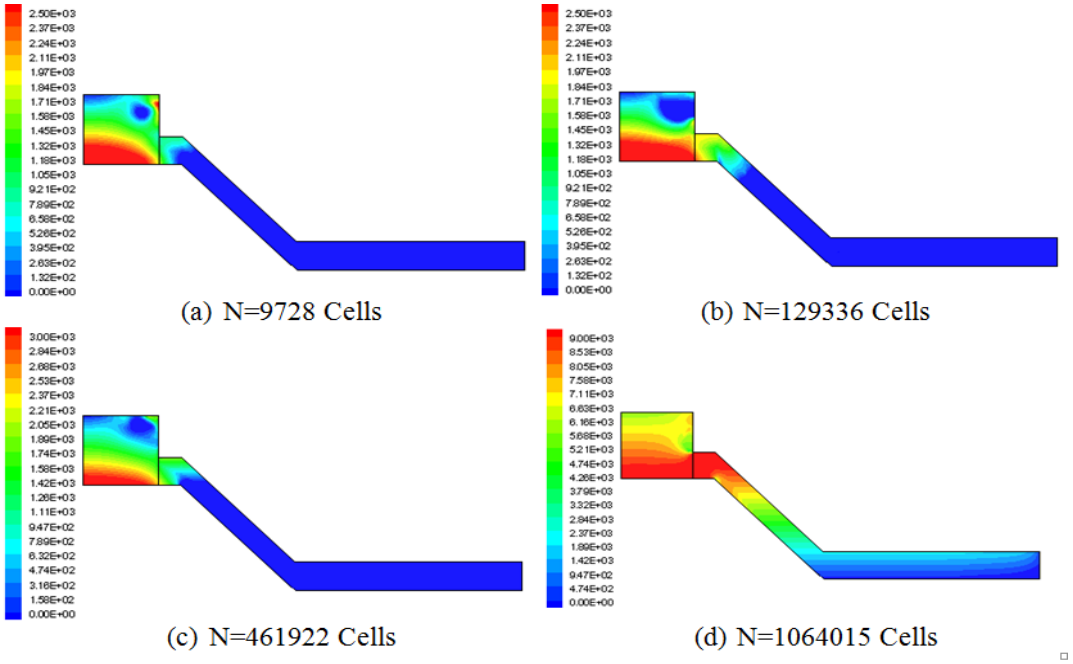

Fig.9Distribution of the static pressure in the plane z=0.5 m at t=1 s

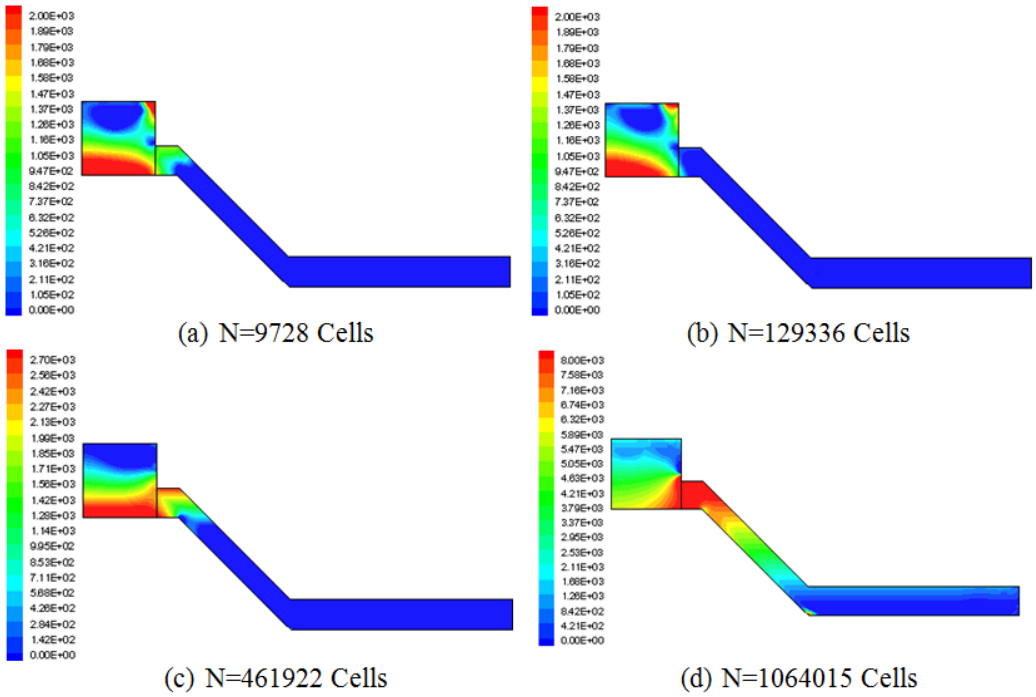

Fig. 10Distribution of the static pressure in the plane z=0.5 m at t=1.4 s

3.3. Dynamic pressure

Figures 11, 12, 13 and 14shows the distribution of dynamic pressure in the test bench on the transverse plane defined by z=0.5 m for the four case of meshing number and for different

instances of the water flow. Dynamic pressure is the component of fluid pressure that represents fluid kinetic energy so it represents the dynamic effects of flow. According to the results, it has been noted that the dynamic pressure has approximately the same behaviors the magnitude velocity. This is because these two parameters are mathematically linked. It has been observed also that the maximum values of dynamic pressure increase when the number of cells increases. For example, at t=1.4s, the dynamic pressure is equal to p_d=5000 Pa for N=9728 cells. But it is equal to P_d=8500 Pa for N=1064015 cells. According to these results, it has been observed that the dynamic pressure in the intake has very weak value during the water flow. In fact, the water height decreases slowly. At the penstock inlet, the dynamic pressure has a maximum value in the water front. When the water front ahead from the penstock to the test section, a progressive increase of the dynamic pressure has been observed.

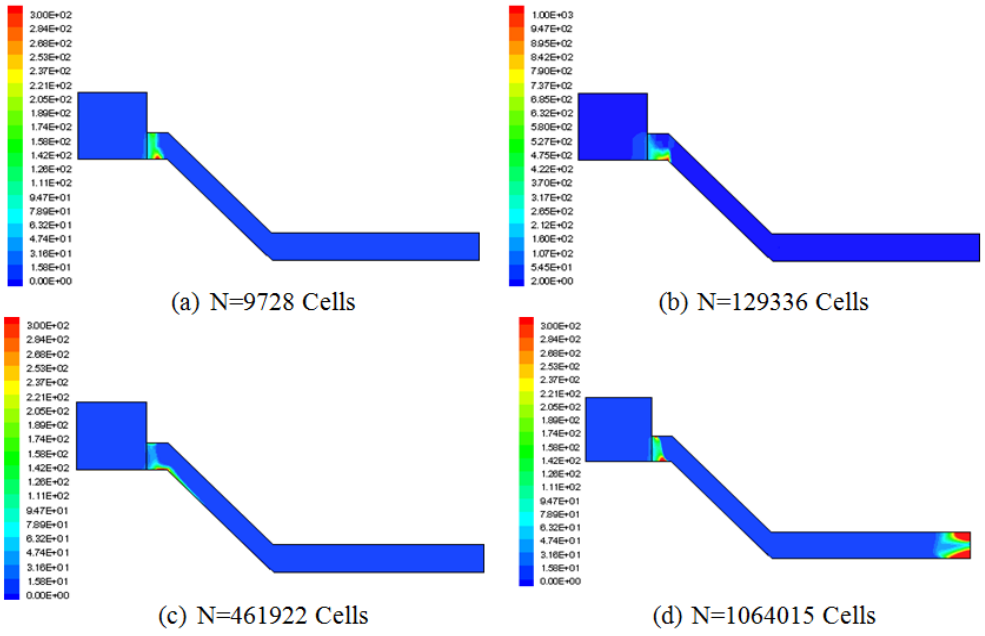

Fig.11Distribution of the dynamic pressure in the plane z=0.5 m at t=0.1 s

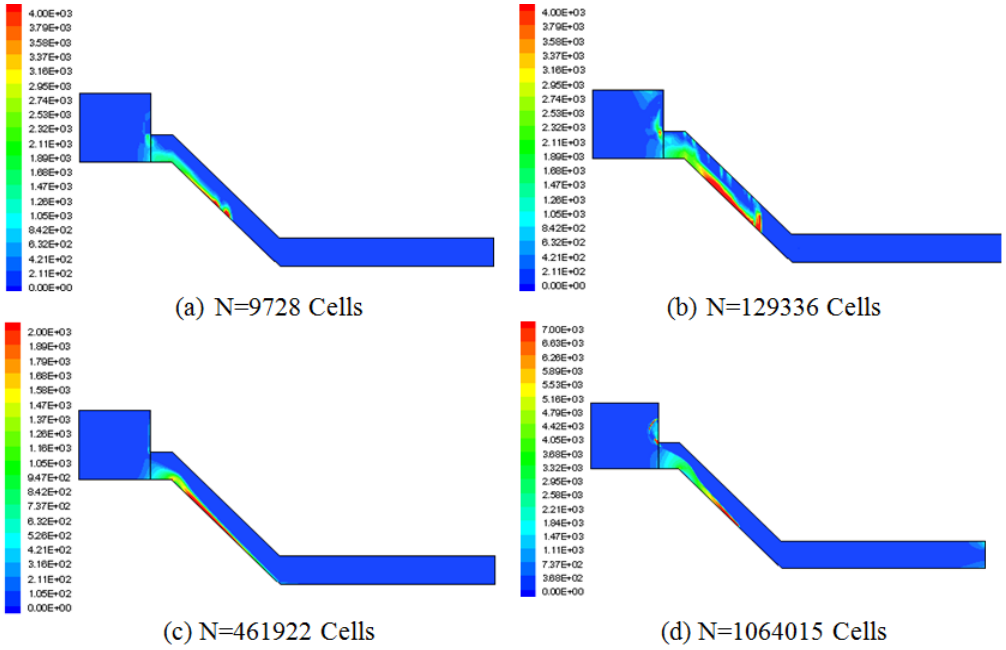

Fig. 12Distribution of the dynamic pressure in the plane z=0.5 m at t=0.6 s

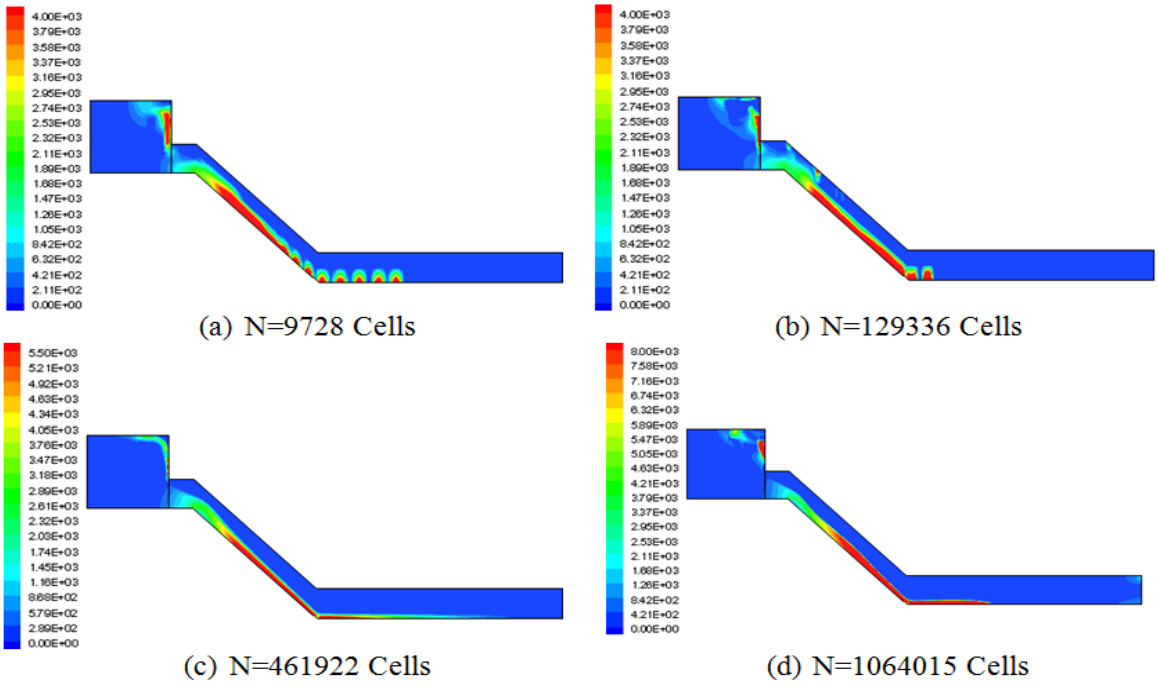

Fig. 13Distribution of the dynamic pressure in the plane z=0.5 m at t=1 s

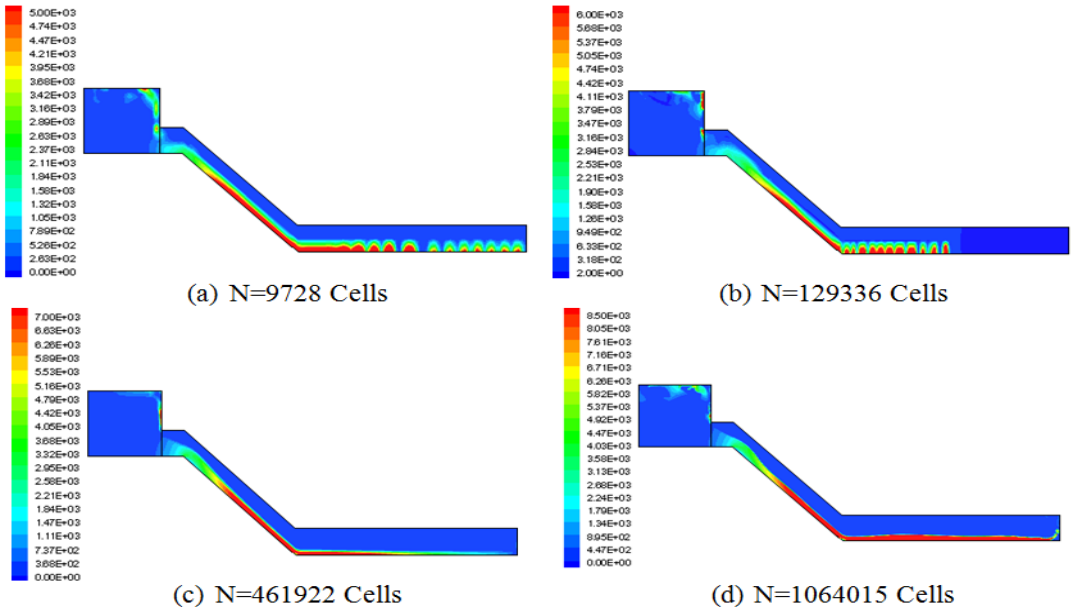

Fig. 14Distribution of the dynamic pressure in the plane z=0.5 m at t=1.4 s

3.4. Free Surface

In this section, we are interested on introducing the effect of number cells in the CFD model. For the case, we have chosen four different numbers of cells and have represented the curve of free surface at 4 different cases in each time.Figures26, 27, 28 and 29represent the surface separating the water from the air for the four cases of meshing number and for different instant of the water flow (3D view). From these results presented below, it can be concluded that in the case having the highest number of cells the longest water front and the highest water level. Indeed, this result is more realistic in the turbulence phenomenon have been appeared.

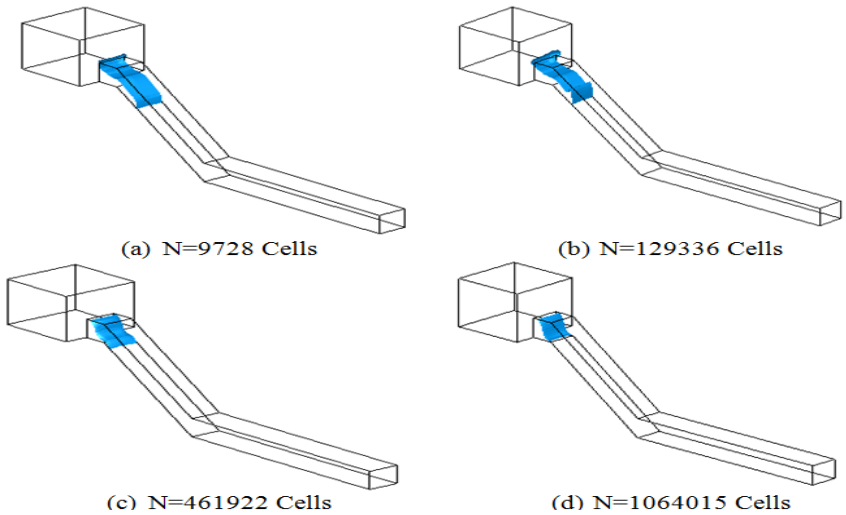

Fig.26 Free Surface at t=0.1 s (3-D view)

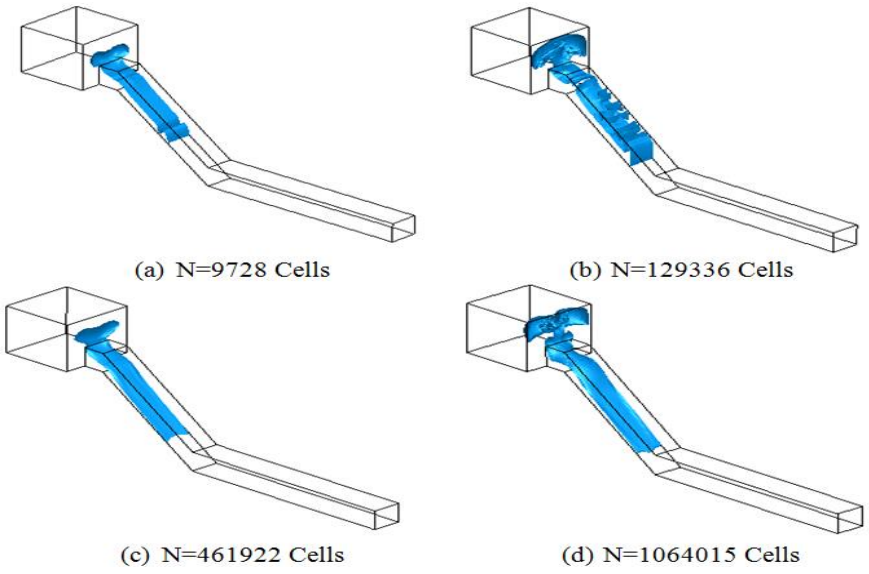

Fig.27 Free Surface at t=0.6 s (3-D view)

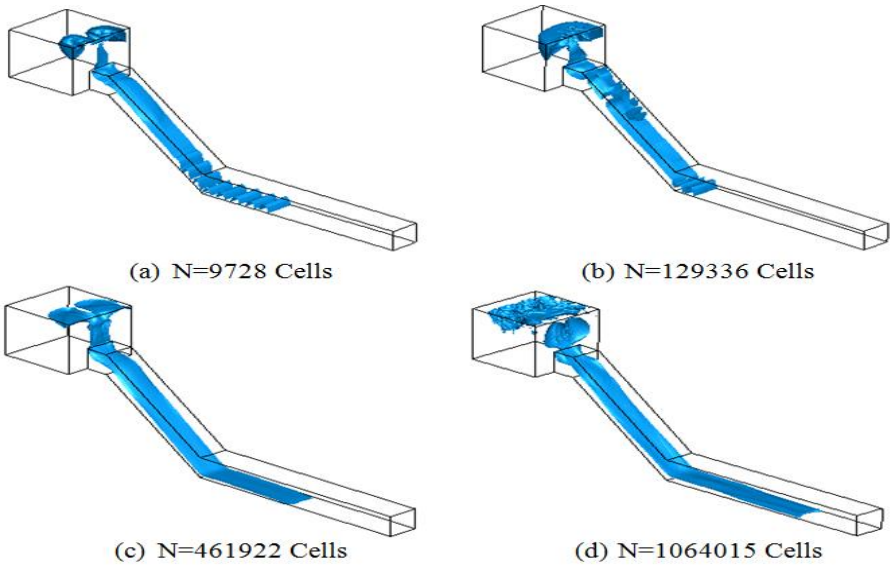

Fig. 28 Free Surface at t=1 s (3-D view)

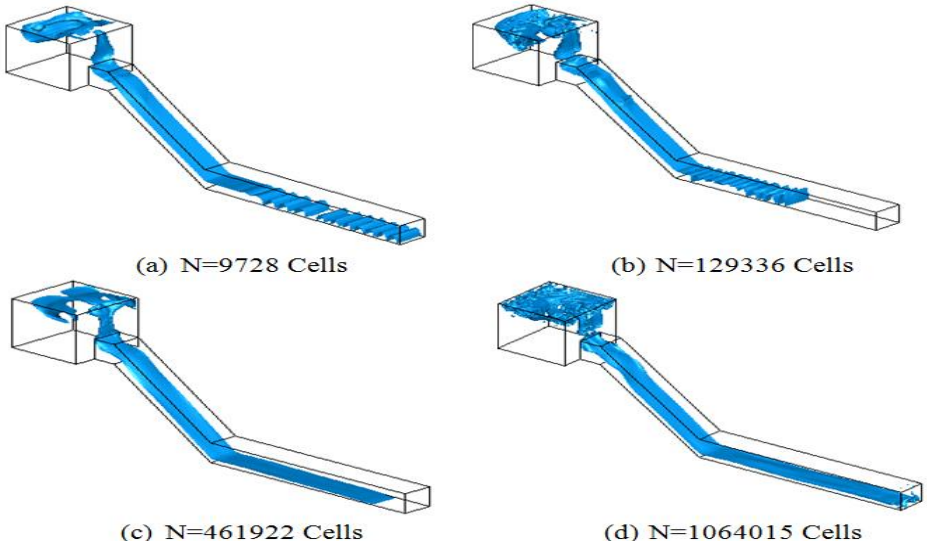

Fig. 29 Free Surface at t=1.4 s (3-D view)

3.5. Comparison with experimental results

3.5.1. Free surface

After testing different numerical model of the water flow in our test bench, we have managed to perform an experience in order to observe the water flow and compare it with our numerical results. Figure 35 present a global view of the experience stuff used during this part. We have managed also to calculate the difference of altitude of water using a Pitot tube in order to determinate the magnitude velocity in several points. The dispositive used is shown in figure 30.

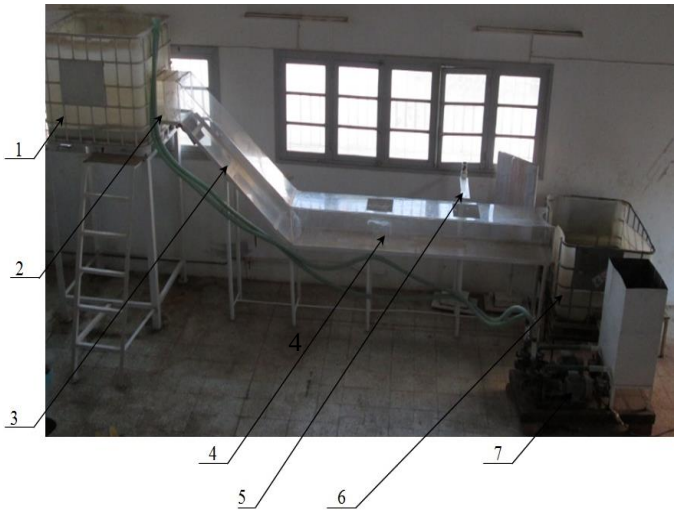

Ref.	Nomenclature
1	Intake
2	Control Gate
3	Penstock
4	Test section
5	Support
6	Outflow
7	Pump

Fig. 30Hydrodynamic test bench

In this section, we are going to compare the previous numerical results with those picked up from experience in order to show the best model approaching the real water behavior. These figures present a superposition of the curves of free surface of experimental and numerical results at 4 times. According to the results presented in these figures, it can be concluded that the numerical results developed with the 1064015 cells model is the best. In fact, a similarity with the experimental free surface curve is presented. Nevertheless, it is very hard, impossible even, to have results exactly similar to the experimental results due to the diversity of factors influencing the water behavior such as the turbulence model or the interaction between water and wall (figure 31).

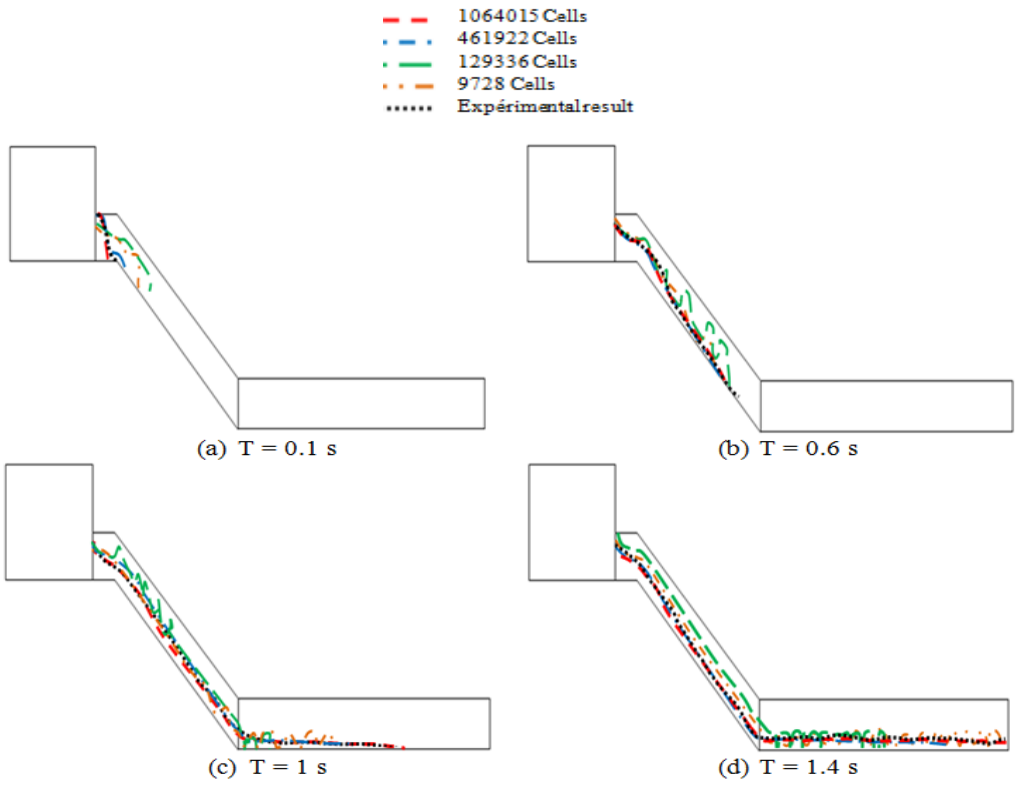

Fig. 31 Comparison with experimental free surface results

3.5.2. Velocity magnitude

Figure 32 shows the different profiles of the velocity magnitude for different cells number. The superposition of the numerical results gathered from the CFD code “Fluent” and the experimental results taken by the Pitot tube shows very good agreements with the 1064015 cells number model. The line considered is situated in the downstream of the test formed by

several point going from z = 0.3 m to z = 0.7 m. In these conditions, y is fixed at -1.4 m and x is fixed at 4.8 m at t = 1.4 s. In the further study, we will adopt these parameters.

Fig. 32Hydrodynamic test bench with Pitot tube

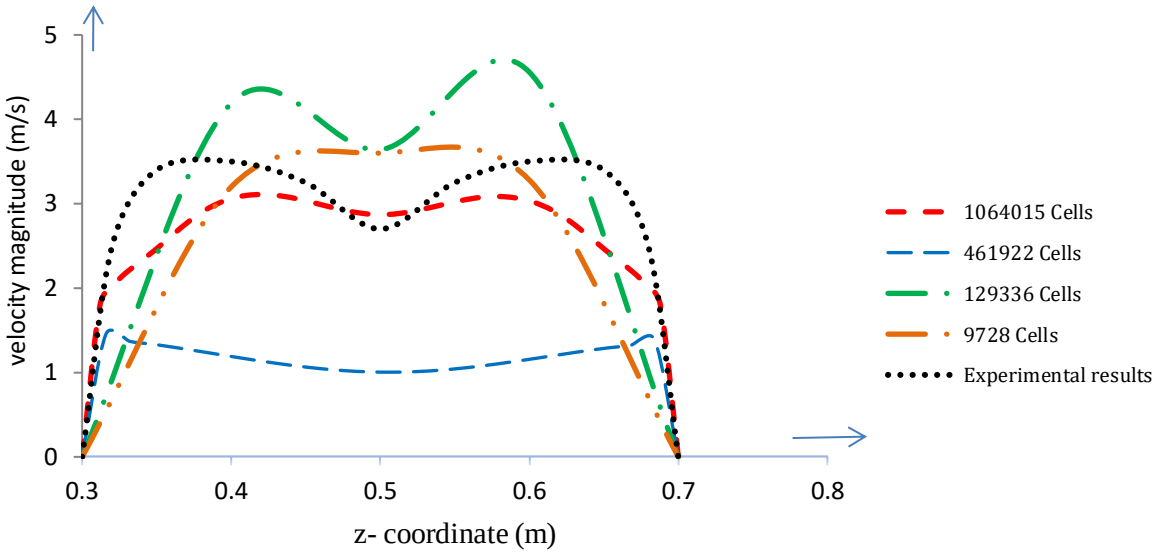

Fig. 33 Comparison of the velocity profiles

4. Conclusion

Savonius rotors in a water channel show promising hydrodynamic behavior with good agreement to literature when modeled with unsteady Navier–Stokes equations using a finite volume approach on a hexahedral mesh; the study compares four mesh densities and reports

favorable accuracy and behavior consistency. Below is a concise guide to understanding and evaluating such simulations. Savonius rotor: a vertical-axis turbine with typically two or three scooped blades that harvests energy from cross-flow; in water, viscous, unsteady effects and vortex structures dominate rotor performance. Computational approach: unsteady Reynolds-averaged Navier–Stokes (URANS) or similar LES-like frameworks solving momentum transport; finite volume discretization on a structured hexahedral mesh is common for stability and accuracy in complex wakes. Mesh design: a mesh with several node/cell counts is used to study mesh independence; typically, finer meshes capture tip vortices and separation regions more accurately at the cost of compute time. Torque and power coefficients: assess average and peak values over rotor rotation, including start-up behavior and torque pulsations. Flow fields: velocity and pressure distributions around blades, wake structures, and recirculation zones, especially in the blade joints and concavities. Numerical and experimental validation: good agreement often indicated by matching averages of torque, power, and rotor efficiency at representative tip-speed ratios and Reynolds numbers.

References

[1] Khan, MJ, B huyan, G, Iqbal MT, Quaicoe, JE, Hydrokinetic energy conversion systems and assessment of horizontal and vertical axis turbines for river and tidal applications: a technology status review. Appl Energy, 86, 1823–35.

[2] Vermaak, HJ, Kusakana, K, Koko, SP, Status of micro-hydrokinetic river technology in rural applications: a review of literature, Renew Sustain Energy Rev, 2014, 29:625–33.

[3] Kari, S, Small scale water current turbines for river applications, Zero Emission Research Organization, Report January 2010.

[4] Ramos, V, Iglesius, G, Performance assessment of tidal stream turbines a parametric approach, Energy Convers Manage 49–57.

[5] Carballo R, Iglesius G. A methodology to determine the power performance of wave energy converters at a particular coastal location.

Energy Convers Manage, 8–18.

[6] Malipeddi AR, Chatterjee D. Influence of ductgeometry on the performance of Darrieus hydro-turbine. Renewable Energy, 292–300.

[7] Ponta, F, Dutt GS, Animproved vertical-axis water-current turbine incorporating a channeling device, Renewable Energy, 20-41.

[8] Bhutta MMA, Hayat N, Farooq AU, Ali Z, Jamil R, Hussain Z. Vertical axis wind turbine – a review of various configurations and design techniques. Renew Sustain Energy Rev, 16–39.

[9] Golecha K, Eldho TI, Prabhu SV. Influence of the deflector plate on the performance of modified Savonius hydrokinetic turbine, Appl Energy, 88 3207–17.